Grazing Incidence X-Ray Photoelectron Spectroscopy: A Method to Study Gate Dielectric Films on Si

Terrence Jach and Eric Landree

Chemical Science and Technology Laboratory, National Institute of Standards and Technology, Gaithersburg, MD 20899, USA

(Received February 27, 2002; accepted March 21, 2002)

Grazing Incidence X-ray Photoelectron Spectroscopy (GIXPS) is a method that offers promise as a non-destructive technique to measure the thickness and chemistry of ultrathin gate dielectric films. It combines aspects of x-ray reflectivity and conventional x-ray photoelectron spectroscopy (XPS). Collimated x-rays are incident on the sample at a grazing angle. A series of photoemission spectra are obtained over a range of incidence angles in the vicinity of the critical angle for total external reflection. The advantage of this method is the incorporation of the optical constants of the layers, as well as the photoemission cross sections of the elements and the inelastic attenuation lengths of the escaping photoelectrons, to fit the nonlinear variation of the photoemission spectra as a function of angle. The x-ray field variation with angle within individual layers provides additional constraints beyond standard angle-resolved XPS for interpreting the densities and thicknesses of multiple layers. The application of this method to the analysis of oxide on Si is described.

1. Introduction

Grazing Incidence X-ray Photoelectron Spectroscopy (GIXPS), also known as Total Reflection X-Ray Photoelectron Spectroscopy (TRXPS), was proposed thirty years ago and has now reached a level of acceptance as a useful surface analysis technique. Both the first experiments and the theoretical analysis were reported by Henke [1]. He envisioned the method as a means to determine better optical constants, x-ray absorption coefficients, and photoelectron mean free paths. Fadley made the observation that the effect of total x-ray reflection in photoemission described by Henke resulted in increases in relative intensities from surface atoms [2,3] Soon thereafter, Mehta and Fadley reported the use of GIXPS for the purpose of measuring the thickness of thin layers on flat surfaces [4] including SiO_2/Si [5]. Other investigators did not go beyond confirming Henke's work [6]. New methods, such as Angle-Resolved XPS (ARXPS), demonstrated enhanced relative surface sensitivity [7], and most layers that were of interest, for example to the thin film or semiconductor industries, were much thicker than the typical escape depths of photoelectrons.

About ten years ago, several factors changed this assessment. Total reflection x-ray fluorescence (TXRF) analysis had become widely used in the semiconductor industry for the investigation of trace contaminants [8], the technology to produce multilayer films had been developed, and x-ray reflectivity (XRR) became a standard technique for investigating the quality of these films. The development of III-V compounds by the semiconductor industry revived an interest in the chemistry of passivation layers. Finally, gate oxide layers on CMOS devices began to approach 10 nm thickness.

At that time Kawai *et al.* showed that in addition to the surface sensitivity and the enhanced surface signal of TRXPS, the inelastic background was highly attenuated for grazing incidence x-rays, provided that samples were extremely flat [9]. In experiments which monitored sample current, Kawai and his coworkers demonstrated that photocurrent yields followed the integrated surface x-ray fields expected in total reflection [10-12].

Chester and Jach demonstrated that GIXPS had an advantage over ARXPS when the specimen surface consisted of multiple thin layers, because the different x-ray optical constants of the layers provide multiple physical constraints beyond the effect of modifying a simple exponential attenuation depth [13]. Chester *et al.* demonstrated GIXPS applied to the study of oxidation states of GaAs with depth [13,14]. Jach and coworkers have described GIXPS systems for use both in

the laboratory and at synchrotron light sources [15-17].

GIXPS has been used to enhance the measurement of metal oxides [18,19], and organic overlayers [20,21] and submonolayer films[22]. It has been incorporated into the measurement of photoemission from multi-layers [23-26], and, as envisaged by Henke, the determination of inelastic electron attenuation lengths [27]. Iijima, Miyoshi, and Saito have demonstrated that GIXPS is capable of monitoring surface impurity concentrations at levels which approach the sensitivity of TXRF [28,29]. Finally, GIXPS has been selected as a process diagnostic method in the development of 400 mm Si wafer technology [30,31].

The indices of refraction of semiconductors and their oxides in the x-ray energy range 1-2 keV frequently differ by significant amounts. When combined with large chemical shifts in XPS and the general flatness of semiconductor substrates, the determination of the chemical state and thickness of semiconductor oxides has proven to be a major application of GIXPS [32-34]. The thickness of gate oxides for CMOS applications has decreased below 10 nm, which is ideally matched to the sampling depth of GIXPS. We describe an example of such a measurement here.

GIXPS has also been applied to the analysis of more complex multilayer oxynitrides on Si [35]. This becomes important as the semi-conductor industry evolves to other gate dielectrics for CMOS applications

2. Method

While GIXPS may be carried out using a laboratory source, synchrotron radiation beamlines optimized for low energy x-rays offer many advantages. Fig. 1 shows the schematic diagram of the configuration used to perform GIXPS on the X-24A beamline at the National Synchrotron Light Source, Brookhaven National Laboratory. This beamline uses a vertically focusing premirror in front of the double-crystal monochromator and a focusing mirror after the monochromator (not shown for clarity). The monochromator consists of an InSb(111)/KDP(200) crystal pair to give a measured energy resolution of 0.4 eV at 1820 eV [36]. A beam of approximately 10^{10} photons/s is focused down to a spot size of 1 mm at the sample. The beam is limited by slits upstream of the monochromator so that the divergence of the beam at the sample was $\Delta\varphi$=0.9°. The beam

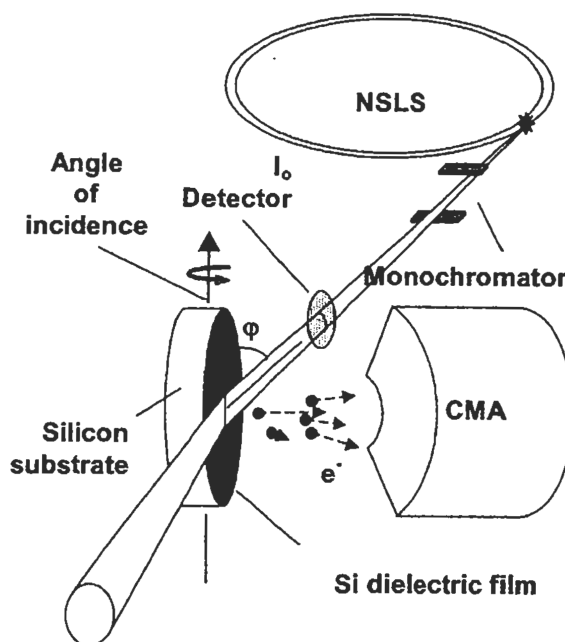

Fig. 1 Diagram of the X-24A beamline configured for GIXPS at 1820 eV.

intensity is monitored by means of the photocurrent from a biased grid upstream of the sample.

Samples of Si wafer of approximately 2 cm × 2 cm dimensions are mounted in an ultra-high vacuum (UHV) chamber containing a precision 2-axis goniometer. The electron spectrometer is a double-pass cylindrical mirror analyzer (CMA) operated at a pass energy of 50 eV, which gives an 800 meV energy resolution.

The sample described here consisted of a thin thermally-grown oxide on a Si wafer which was being used as an intercomparison with ellipsometry. The sample was protected by photoresist which was removed just before mounting in the UHV chamber. The chamber was baked at 100°C before the measurement. Measurements were made at pressures between 2.7×10^{-7} Pa and 2.7×10^{-8} Pa (2×10^{-9} and 2×10^{-10} Torr). Preliminary XPS spectra showed that a C overlayer was the only contamination present. C is invariably present, both as a residual contamination from transfer of the sample as well as from incomplete removal of the photoresist protective layer.

The critical angle for total reflection from Si at 1820 eV is φ_c=0.7°. Spectra were taken of the Si 2p, O 1s, and C 1s photoemission lines at 0.1° intervals for angles of incidence from 0° to 1.5°. The spectra were taken at intervals of 0.2 eV at 3s per point. The entire

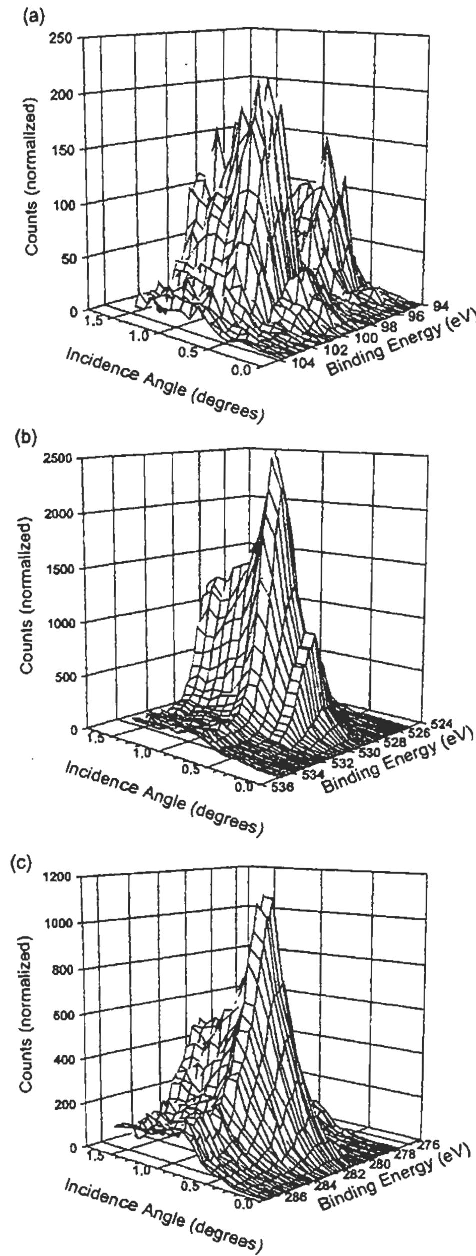

Fig. 2 GIXPS of an SiO_2/Si sample; spectra taken as a function of the angle of incidence: (a) Si 2p, (b) O 1s, and (c) C 1s.

set of photoemission spectra required approximately 3 hours.

3. Data Analysis

The data are shown in Fig. 2(a-c). The 3-D plots show spectra plotted as counts normalized to the synchrotron beam intensity vs. binding energy and angle of incidence.

Our data analysis consists of a two-step process. First, the peaks due to photoemission from the Si 2p level in Si, Si 2p in SiO_2, the O 1s in SiO_2, and the C 1s in the C overlayer are fitted to obtain integrated intensities at each angle. The fits take into account the energy, width, asymmetry, Gaussian-Lorentzian shape of the photoemission peaks, and the inelastic background which must be included in the total photoemission yield.

The integrated yields as a function of incidence angle are then subjected to a second fit procedure which determines individual layer thicknesses and ordering. The model assumes homogeneous layers with sharp interfaces, uniform densities, and well-defined optical constants. In this case, we take the system to be a Si substrate, an SiO_2 overlayer, and an amorphous carbon surface reacted with O to the extent observed (10%) in the C 1s photoemission [37].

The fit procedure uses a least squares fit of all the line yields, weighted according to their relative intensities, at all incidence angles, to determine the thickness of the C and SiO_2 layers. The fit procedure takes into account the correlation with angle which must exist between the components of the same layer—one of the principle constraints of the method. The x-ray field in each layer is calculated using a recursion method of Parratt [38], but adapted for large angles using the formulation of de Boer [39]. The resulting x-ray photoemission yield from an element e in a system of l layers (including the substrate) is given by:

$$Y_e = \sum_j \frac{FS}{2Z_0 hc} \rho_{ej} \sigma_e e^{-\frac{1}{\cos\theta}\sum_{l<j}\Gamma_l d_l}$$

$$\times \int_0^{d_j} dz_j \left(\left|E_j\right|^2 e^{-\frac{4\pi}{\lambda}N''_{jz} z_j} + \left|E_j^R\right|^2 e^{\frac{4\pi}{\lambda}N''_{jz} z_j} + \left|E_j E_j^{R*}\right| \cos\left(\alpha_j + \frac{4\pi}{\lambda}N''_{jz} z_j\right)\right) e^{-\frac{\Gamma_j}{\cos\theta} z_j} \quad (1)$$

where E_j and E_j^R are the fields due to the incident and reflected beam in the jth layer ($0 \le j \le l$) and $\alpha_j = \tan^{-1}\left(\mathrm{Im}\left(E_j^* E_j^R\right)/\mathrm{Re}\left(E_j^* E_j^R\right)\right)$ is the phase angle between the fields. N_{jz} is the z component of the complex vector of refraction $N_j = N_j' - iN_j''$ in an absorptive medium for x-rays of wavelength λ [40]. The quantities ρ_{ej} and σ_e are respectively the atomic density of the element e in the jth layer and the photoemission cross section for the particular

subshell under consideration. The factor F takes into account the solid angle acceptance and collection efficiency of the electron spectrometer, and S is the area of the sample. The portion of the sample observed by the electron spectrometer appears to be uniformly illuminated by the beam at all angles. Γ_j is the Mean Escape Depth (MED) of the photoelectrons in the jth layer and θ is the takeoff angle of the electron spectrometer from the surface normal. The thickness of the jth layer is d_j and $Z_0 = \sqrt{\mu_0 / \varepsilon_0}$.

The fits require a number of physical parameters as inputs. We use subshell photoemission cross-sections [41], indices of refraction [42], and MED's corrected for elastic scattering [43]. We assumed a density of 2.33 g/cm^3 for the Si substrate, 2.27 g/cm^3 for the SiO_2 layer, and 2.00 g/cm^3 for the C overlayer. We also assumed that the efficiency of the CMA is given by the standard expression [44].

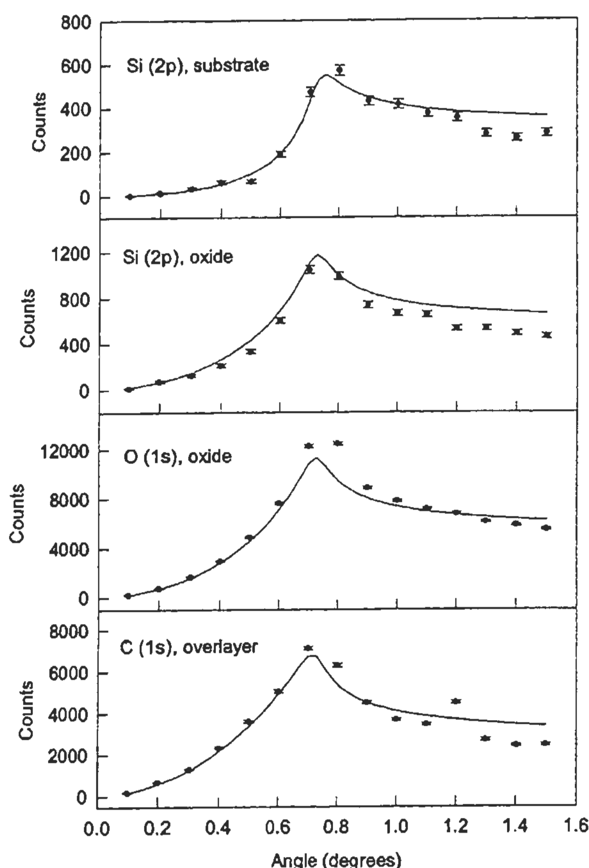

Fig 3. Photoemission yields (data points) and fits (solid lines) as a function of angle of incidence for Si 2p (substrate), Si 2p (SiO_2), O 1s (SiO_2), and C 1s (overlayer). The error bars are due to count statistics

4. Results and Discussion

The GIXPS photoemission yields as a function of angle of incidence and the best fits to the yields are shown in Fig. 3. The best fit for the sample described here gives a thickness of the oxide layer of 4.4±0.7 nm for the SiO_2 layer and 1.6±0.25 nm for the amorphous C overlayer. The error limits on the layers were set after an assessment of the potential errors in the physical parameters, of which the uncertainty in the optical constants is the largest [45]. They are considerably smaller than the variations in thickness obtained from other methods of measuring SiO_2/Si in this thickness range [46]. The overall accuracy of GIXPS measurements with synchrotron radiation is expected to improve as better error limits are established for the physical parameters used in fitting data taken with incident energies between 1 and 2 keV.

The effects of surface and interface roughness and graded interfaces have been discussed elsewhere [45]. At the wavelength of the incident x-rays, λ=6.8Å, the SiO_2/Si surface and interface look smooth and abrupt. Graded interfaces give an average value for the thickness.

In summary, we have described here the applications in which GIXPS has been used and the method by which it may currently be carried out. GIXPS is an analytical method which has the advantage of providing chemical and thickness information on samples whose surfaces consist of multiple thin layers. As such, GIXPS is highly suitable for the analysis of the chemical and physical characteristics involved in gate dielectric fabrication.

5. Acknowledgments

Part of this research was carried out at the National Synchrotron Light Source, Brookhaven National Laboratory, which is supported by the U.S. Department of Energy, Division of Materials Sciences and Division of Chemical Sciences, under Contract No. DE-AC02-98CH10886

References

[1] B. L. Henke, Phy. Rev. A **6**, 94 (1972).
[2] C. S. Fadley, R. J. Baird, W. Siekhaus, T. Novakov, and S. A. L. Bergström, J. Electron Spectrosc. **4**, 93 (1974).

[3] C. S. Fadley, J. Electron Spectrosc. **5**, 725 (1974).
[4] M. Mehta and C. S. Fadley, Phys. Lett. **55A**, 59 (1975).
[5] M. Mehta and C. S. Fadley, Chem. Phys. Lett. **46**, 225 (1977).
[6] M. V. Kruglov and I. K. Solomin, Sov. Phys. Solid State **28**, 1436 (1986).
[7] M. Pijolat and G. Hollinger, Surf. Sci. **105**, 114 (1981).
[8] R. Klockenkamper, "Total-Reflection X-Ray Fluorescence Analysis", J. Wiley & Sons, New York, 1996.
[9] J. Kawai, M. Takami, M. Fujinami, Y. Hashiguchi, S. Hayakawa, Y. Gohshi, Spectrochim. Acta, **47B**, 983 (1992).
[10] J. Kawai *et al.*, Appl. Phys. Lett. **63**, 269 (1993).
[11] J. Kawai *et al.*, Proc. Japan Acad. **69B**, 179 (1993).
[12] J. Kawai, S. Hayakawa, Y. Kitajima, and Y. Gohshi, Anal. Sci. **11**, 519 (1995).
[13] M. J. Chester and T. Jach, Phys. Rev. B **48**, 17262 (1993).
[14] M. J. Chester, T. Jach, and S. Thurgate, J. Vac. Sci. Technol. B **11**, 1609 (1993).
[15] T. Jach and S. M. Thurgate, U. S. Patent 5,280,176 (1994).
[16] T. Jach, M. J. Chester, and S. M. Thurgate, Rev. Sci. Instrum. **65**, 339 (1994).
[17] T. Jach, M. J. Chester, and S. M. Thurgate, Nucl. Instrum. Methods A **347**, 507 (1994).
[18] K. Nisawa and K. Okuda, J. Surf. Anal. **1**, 213 (1995).
[19] K. Hayashi *et al.*, Advances in X-ray Chem. Anal. Japan **28**, 53 (1997).
[20] J. Kawai, S. Kawato, K. Hayashi, T. Horiuchi, K. Matsushige, and Y. Kitajima, Appl. Phys. Lett. **67**, 3889 (1995).
[21] K. Hayashi, J. Kawai, S. Kawato, T. Horiuchi, K. Matsushige, and Y. Kitajima, Advances in X-ray Chem. Anal. Japan **28**, 45 (1997).
[22] W. Drube, T. M. Grehk, R. Treusch, and G. Materlik, J. Electron Spectrosc. **88-91**, 683 (1998).
[23] K. Hayashi *et al.*, Appl. Phys. Lett. **68**, 1921 (1996).
[24] H. Amano, J. Kawai, K. Hayashi, and Y. Kitajima, Advances in X-ray Chem. Anal. Japan **28**, 31 (1997).
[25] J. Kawai, H. Amano, K. Hayashi, T. Horiuchi, K. Matsushige, and Y. Kitajima, Spectrochim. Acta B **52**, 873 (1997).
[26] J. Kawai, K. Hayashi, H. Amano, H. Takenaka, and Y. Kitajima, J. Electron Spectrosc. **88-91**, 787 (1998).
[27] J. Kawai, H. Adachi, Y. Kitajima, K. Maeda, S. Hayakawa, and Y. Gohshi, Anal. Sci. **13**, 797 (1997).
[28] Y. Iijima, K. Miyoshi, and S. Saito, JEOL News **33E**, 20 (1998).
[29] Y. Iijima, K. Miyoshi, and S. Saito, Surf. Interface Anal. **27**, 35 (1999).
[30] H. Yamagishi *et al.*, Microelectronic Eng. **45**, 101 (1999).
[31] M. Mayusumi, M. Imai, J. Takahashi, K. Kawada, and T. Ohmi, J. Electrochem. Soc. **146**, 2235 (1999).
[32] J. Kawai, S. Hayakawa, Y. Kitajima, K. Maeda, and Y. Gohshi, J. Electron Spectrosc. **76**, 313 (1995).
[33] T. Jach, S. Thurgate, and T. LaCuesta, in "Semiconductor Characterization: Present Status and Future Needs," W. M. Bullis, D. G. Seiler, and A. C. Diebold, eds., American Institute of Physics, New York, 1996, p. 283.
[34] T. Jach, J. Gormley, and S. Thurgate, Spectrochim. Acta B **54**, 1539 (1999).
[35] E. Landree *et al.*, in "Characterization and Metrology for ULSI Technology: 2000 International Conference," D. G. Seiler, A. C. Diebold, T. J. Shaffner, R. McDonald, W. M. Bullis, P. J. Smith, and E. M. Secula, eds., American Institute of Physics, New York, 2001, p. 159.
[36] B. A. Karlin, J. C. Woicik, and P. L. Cowan, Nucl. Instrum. Methods A **347**, 360 (1994).
[37] J. R. Shallenberger, D. A. Cole, D. F. Downey, and Z. Zhao, in "Proceedings of the XII International Conference on Ion Implantation Technology," J. Matsuo, G. Takaoka, and I. Yamada, eds., IEEE, 1998.
[38] L. G. Parratt, Phys. Rev. **95**, 359 (1954).
[39] D. K. G. de Boer, Phys. Rev. B **44**, 498 (1991).
[40] M.-R. Lefévère, and M. Montel, Opt. Acta **20**, 97 (1973).
[41] J. H. Scofield, Report UCRL-51326, Lawrence Livermore Laboratory, 1973.
[42] B. L. Henke, E. M. Gullikson, and J. C. Davis, At. Data Nucl. Data Tables, **54**, 181 (1993).
[43] A. Jablonski, C. J. Powell, J. Vac. Sci. Technol. A **15**, 2095 (1997).
[44] M. P. Seah, Surf. Interface Anal. **20**, 243 (1993).
[45] T. Jach and E. Landree, Surf. Interface Anal. **31**, 768, (2001).
[46] D. A. Cole *et al.*, J. Vac. Sci. Technol. B **18**, 440 (2000).